MAGNETIC FIELD MEASUREMENTS OF THE Nb_3Sn COMMON COIL DIPOLE RD3C

L. Chiesa[#], S. Caspi, D.R. Dietderich, P. Ferracin, S.A. Gourlay, R.R. Hafalia, A.F. Lietzke, A.D. McInturff, G. Sabbi and R.M. Scanlan, LBNL, Berkeley, CA 94720, USA

Abstract

Goal of the LBNL Superconducting Magnet Program is to establish the technologies associated with very high field superconducting magnets, to provide cost-effective options for the next generation of high-energy colliders. Recent efforts have focused on the design, fabrication and test of Nb_3Sn common coil dipoles. The RD3b test has demonstrated operation at very high field and stress levels. RD3c is the first common coil prototype addressing field quality issues. A flat racetrack coil was wound on both sides of a central bore plate, using hard spacers to control the geometric field harmonics. The resulting coil module was inserted between the outer coil modules of RD3b, and pre-stressed using the reusable yoke and shell loading structure. In this paper, magnetic field measurements of RD3c are reported and compared with theoretical predictions.

INTRODUCTION

Magnet parameters

RD3c was conceived as a simple coil configuration that would test the capability to obtain geometric field quality in the range required for high energy accelerators. RD3c was composed of RD3b's outer coils, yoke and shell structure [1-3] and a new inner coil, clamped between the two outer coils [4]. In Table 1 the RD3c performance parameters are listed.

Table 1: RD3c Performance Parameters

$I^{(ss)}$ (kA)	11.9
$B_0^{(ss)}$ (T)	10.9
$J_{cu}^{(ss)}$ (inner) (kA/mm^2)	1.6
$J_{cu}^{(ss)}$ (outer) (kA/mm^2)	1.6

* Calculated values. Training was suspended before maximum current was achieved.

The new inner module was composed of two single-layer coils, with one spacer per layer. The two layers were wound on both sides of two central bore plates and connected by an S-bend ramp through the island-pole. The spacers near each borehole allowed enhancing the field quality by compensating the large positive sextupole generated by the outer coils. The design was not optimized to correct the end field and the iron saturation harmonics. As in RD3b, the inner coils were separated by an aluminum-bronze bore-plate. A thicker mid-plane bore-plate was designed to contain the 35 mm bore and allow the insertion of a 25 mm diameter, rotating-coil probe. Fig. 1 shows the cross section of RD3c.

* This work was supported under contract DE-AD03-76SF00098 by the Director, Office of Energy Research, Office of High Energy Physics, U.S. Department of Energy.

lchiesa@lbl.gov

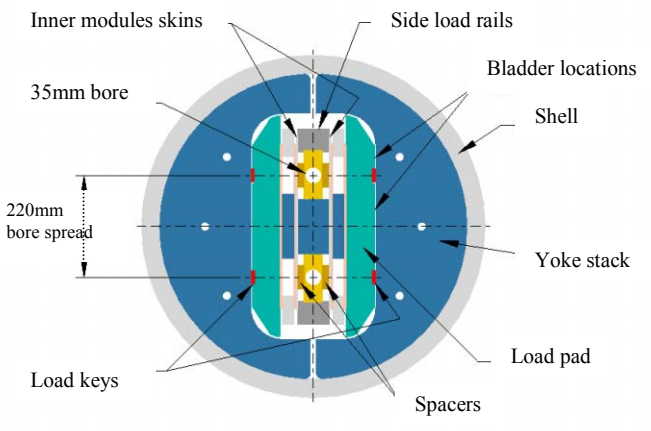

Figure 1: The magnet cross-section for RD3c.

The goal of this magnet was to measure field harmonic data after standard training, quench and ramp rate studies [3]. Training started at 77% of short sample and reached 92%. At this point it was decided to suspend training and perform magnetic measurements.

MAGNETIC MEASUREMENTS RESULTS

Test Set-Up

A rectangular coordinate system is defined by the z-axis at the center of the magnet aperture and pointing from the return end towards the leads end, the x-axis horizontal pointing to the right of an observer who faces the leads of the inner module and the y-axis defined by the right hand rule (Fig. 2).

The field is represented in terms of harmonic coefficients defined by the power series expansion shown in equation (1) with r_0 10 mm:

$$B_y + iB_x = B_{ref} \sum_{n=1}^{\infty} (b_n + ia_n) \left(\frac{x+iy}{r_0} \right)^{n-1} \qquad (1)$$

The rotating coil, 428 mm long, has 11.7 mm radius and 5 windings: 1 tangential, 2 dipole bucking, and 2 quadrupole bucking (not used in this test). The dual dipole correction coils were wired to provide a high-resolution harmonic signal by suppressing the fundamental dipole component. The probe rotated at constant speed of 1Hz. Both the tangential and bucked signals were amplified with an integrating amplifier, digitized at 1kHz with 24 bit HP3458A DMV's, and Fourier analyzed relative to the fundamental. The resulting harmonics were corrected for the appropriate amplifier gain and coil harmonic sensitivities, and normalized to a radius of 10 mm to compare them with the calculations.

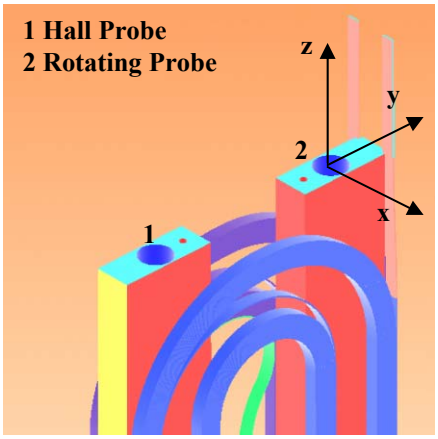

Figure 2: RD3c inner module and definition of coordinate system.

A Hall probe was inserted in the other bore for an independent measurement of the dipole field.

Magnet field quality

Four current cycles were applied to the magnet, in order to measure the hysteresis harmonics. The central 43 cm integral harmonics were measured on the fly during the cycles.

A first set of measurements (MM03) was obtained during the first and second cycles and a second set of measurements (MM04) was obtained during the third and fourth cycles. The ramp rate was 10 A/s for MM03 and for the first cycle of MM04 and 30A/s for the second cycle of MM04. All ramp cycles, with the exception of the second cycle, went to 10 kA and back, with several pauses to measure the superconductor magnetization. At 10 kA longitudinal scan data were collected. After these measurements were taken the magnet was ramped down to 500 A where the current was held prior to the start of the next cycle. During the cycle with 30 A/s ramp rate, no holds were performed and an entire loop up to 10 kA and down to 0 A was completed.

The normalized allowed central harmonic integrals at 90% of short sample are summarized in Table 2. In the same table the main dipole B1 calculated and measured with the rotating probe and with the Hall probe is shown.

A 5 units difference between the measured normal sextupole and the calculated values was recorded at 10 kA. A 15 units difference was observed for the skew quadrupole. The calculated values of the normal sextupole and skew quadrupole are a consequence of iron and end effects, features not specifically optimized for this test. Since the shift from the expected values is constant with the current (Fig. 5), geometric effects are probably the cause of this difference. Preliminary calculations of the effects of cooldown do not explain this difference. The discrepancy could be explained by effects such as position of supporting pads, displacement of the coils and fabrication tolerances (Table 3). Higher order harmonics are small and in agreement with the calculated values.

The normalized central sextupole for the 10A/s cycles is shown in Fig. 3. At 10 kA a significant hysteresis was still present mainly due to persistent currents effects. The residual hysteris was predicted from 2D calculations, also shown in Fig. 3, based on magnetization data of the strands (courtesy of Ohio State University). The calculated values and measurements were shifted in order to be symmetric around 0 unit at 10 kA. This allowed a better comparison between the 2D calculations and the measurements showing a reasonable agreement of the data with the predicted behavior.

Table 2: Calculated and Measured Main dipole B1 and allowed harmonics at 10kA

Normal	Calc	Meas	Skew	Calc	Meas
b_3	-5.44	-10.39	a_2	-31.2	-15.65
b_5	-0.24	-0.02	a_4	-1.56	-1.45
b_7	0.58	0.61	a_6	0.01	-0.20
B1(T) integrated	9.16	9.77	B1(T) central	9.23	9.26

Measured values: 1E-4 units, averaged between up-ramp and down-ramp to cancel the hysteresis (r_0= 10mm).

Table 3: Sensitivity to geometric effect

Normal sextupole	Value	Δb_3
Inner/outer cable thickness	+10 μm	+0.3/-1.15
Central spacer height	+100 μm	+0.5
Inner/outer coil horiz. position	+100 μm	+0.9/+0.4
Skew quadrupole	Value	Δa_2
Inner/outer coil vert. displac.	+100 μm	+3.0/-2.8

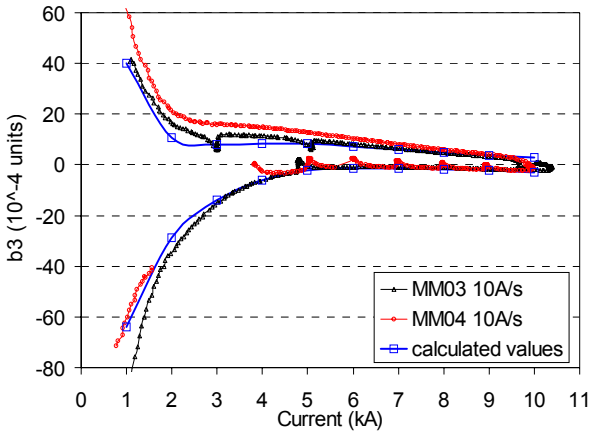

Figure 3: Normal sextupole, 10A/s measurements and 2D hysterisis calculation using magnetization data of strands.

The Hall probe measurements in one bore were compared with the peak central field calculations. For current above 3 kA the measurements agree with the calculated values within 0.5% (Fig. 4). Below 3 kA the discrepancy increases up to 2%. Persistent and eddy current effects are not included in the calculations. In the second bore the measurements of the dipole component performed with the rotating coil were compared with the 3D calculated integrals over the probe-coil length (slightly lower than the central value due to the ends effect). In this case there was a systematic deviation of 5% from the calculated values, which is still under investigation.

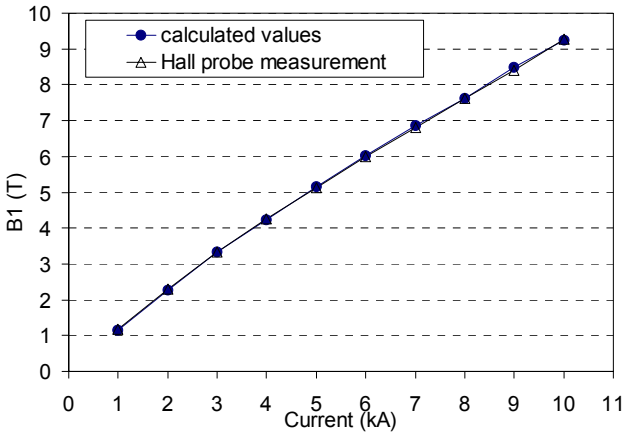

Figure 4: Main dipole component as a function of current.

The geometric normalized sextupole as a function of current is shown in Fig. 5. Up-ramp and down-ramp values were averaged to eliminate ramp rate and magnetization hysteresis. The average of the measurements with its error bars was compared with the calculation. The current dependence of the harmonic value is due to saturation of the iron. The measured normal sextupole well reproduces the expected saturation effect but had a relatively constant shift of 5 units from the absolute value as mentioned earlier.

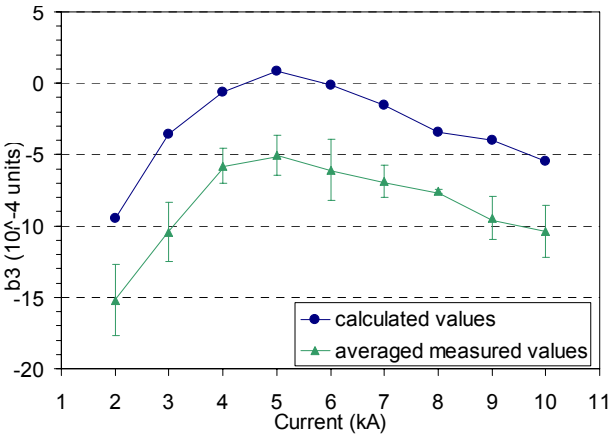

Figure 5: Normalized integrated sextupole as a function of magnet current (data averaged among up-down ramps).

Longitudinal scans were also performed. The measured values of the main dipole field B1 and normal sextupole component were compared with the calculated values. For the main component B1 a scaling factor was applied to account for the 5% B1 error previously discussed. The data also needed to be shifted longitudinally 18 mm relative to the center position, which was determined roughly by oscilloscope measurements. An 18 mm error was well within the uncertainty of this method of positioning. For the sextupole, the expected dependence from position was satisfactory but a negative 5 units shift from the calculated values was again observed Fig. 6.

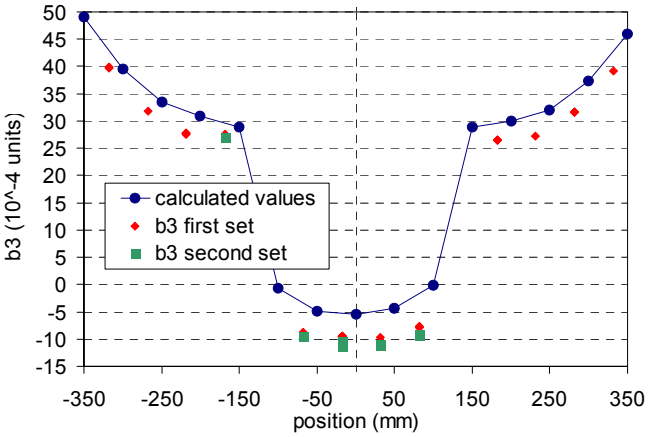

Figure 6: Axial dependence of the sextupole b3 relative to the center of the magnet.

CONCLUSIONS

RD3c was the first high field common coil with basic field quality features. The results obtained in this first attempt were very satisfactory considering the design constrains of the magnet. Several upgrades of the test facility were also implemented for this test (new header and vertical motion apparatus).

Further investigations will be addressed in order to explain the discrepancies between calculation and measurements. A careful analysis of fabrication tolerances and their effect on field quality is required. Possible sources of field error are also the mechanical effects due to deformation of the coil under Lorentz forces at cold compared to the room temperature unstressed geometry, and magnetization effects (visible at low currents). Samples of iron and aluminum-bronze bore plate are being measured at NIST to confirm the permeability values used in the model.

A second thermal cycle with more focused measurements is planned to improve the quality of data collected and increase the statistic of results. It will allow a better understanding of magnetization and eddy current effects and the investigation of snap back behavior in Nb_3Sn magnets.

Common coil designs optimized to address iron saturation and field quality have been developed and will be implemented in future prototypes [6].

REFERENCES

[1] S.A. Gourlay et al., *IEEE Trans. Appl. Superconduc.*, Vol. 11, No. 1, March 2001, p.2164.

[2] A.F. Lietzke et al., "Fabrication and Test Results of a High Field, Nb_3Sn Racetrack Dipole", *Proceedings: 2001 Particle Accelerator Conference*, Chicago, IL, June 2001, p.208.

[3] A.F. Lietzke et al., "Test Results of RD3c, a Nb_3Sn Common-Coil Racetrack Dipole Magnet", *Proceedings: IEEE Trans. Appl. Superconduc.*, Houston, TX, August 2001.

[4] S. Caspi et al., "A New Support Structure for High Field magnets", *IEEE Trans. Appl. Superconduc.*, Vol. 12, No. 1, March 2002, p. 47.

[5] G. Sabbi et al., "Design of Racetrack Coils for High-Field Dipole Magnets", *IEEE Trans. Appl. Superconduc.*, Vol. 11, No. 1, March 2001, p. 2280.